

# Si(100)2×1-Cl structure from x-ray-absorption spectroscopy

D. Purdie,\* N. S. Prakash,<sup>†</sup> K. G. Purcell,<sup>‡</sup> P. L. Wincott, and G. Thornton  
*Interdisciplinary Research Centre in Surface Science and Chemistry Department,  
 Manchester University, Manchester M13 9PL, United Kingdom*

D. S.-L. Law

*Science and Engineering Research Council, Daresbury Laboratory, Warrington WA4 4AD, United Kingdom*

(Received 1 March 1993)

Surface-extended x-ray-absorption fine-structure (SEXAFS) and near-edge x-ray-absorption fine-structure (NEXAFS) spectroscopy at the Cl *K* edge have been used to investigate the structure of Si(100)2×1-Cl. A vicinal single-domain Si(100)2×1 substrate was employed to simplify data analysis. This substrate was exposed to Cl<sub>2</sub> at about 500 K to yield a coverage of about 0.25 monolayers. The room-temperature SEXAFS data indicates that Cl sits atop the upper Si atom of a buckled dimer at a bond distance of 2.00±0.02 Å. Analysis of the polarization-dependent NEXAFS data, which relies on the pseudointramolecular behavior of a  $\sigma^*$  resonance, is consistent with this geometry. However, it is inconsistent with the structural model derived from a recent electron-stimulated-desorption ion-angular-distribution study, in which Cl atoms are bound to both ends of a symmetric dimer. We point out that this discrepancy may arise from a difference in the coverage employed.

## I. INTRODUCTION

Measuring and predicting semiconductor surface reconstructions and their modification by adsorbates present a particularly difficult challenge to current experimental and computational techniques. This arises from their complexity and the small difference in energy of alternative and quite different structures. For the Si(100) surface there has recently been some convergence of experimental and theoretical views. It is now established<sup>1</sup> that the clean surface reconstructs to a  $c(4\times 2)$  net at low temperature (120 K), resulting from the ordering of buckled dimers. Scanning tunneling microscopy (STM) data<sup>1</sup> also suggest that the buckled dimer remains the lowest-energy configuration at room temperature, where a 2×1 symmetry is observed. A recent calculation of the clean surface electronic structure predicts buckled dimers to be 0.14 eV more stable than their symmetric counterparts.<sup>2</sup>

Adsorbates modify the reconstruction, as might be expected given the delicate energy balance between the two dimer structures.<sup>2,3</sup> Here we have in mind electronegative adsorbates of importance in technological processes such as etching, passivation, and interface formation.<sup>3-5</sup> Modifications to the clean surface reconstruction are in some cases observed as changes to the low-energy electron-diffraction (LEED) pattern.<sup>2-5</sup> Other studies have used the dispersion of adsorbate electron bands and changes to the substrate electronic structure to gauge the surface structure.<sup>3</sup> There have been surprisingly few studies which have employed direct probes of the crystallography. The available experimental results for H (Ref. 6) and F (Ref. 7) point to adsorption on both ends of a symmetric dimer, as shown in Fig. 1(a). In contrast, As forms symmetric dimers on top of the Si(100) surface,<sup>5</sup> as shown in Fig. 1(b). The picture for Cl adsorption is controversial.<sup>8-10</sup>

The proposed bonding arrangement of H from scan-

ning tunneling microscopy,<sup>6</sup> and F from the electron-stimulated-desorption ion-angular-distribution,<sup>7</sup> (ESDIAD) is chemically appealing. This has H and F saturating the surface dangling bonds at both ends of a symmetric dimer. Although there are no experimental data for S and Se, local-density-approximation (LDA) calculations<sup>2</sup> predict that they will break the dimer bond and bridge top-layer Si atoms in a 1×1 array. These results are consistent with experimental data for Ge(100)-S.<sup>11</sup> The situation for Cl might be expected to parallel that for H and F, although the possibility of bridge bonding must also be considered. The latter configuration was predicted by SLAB-MINDO (where MINDO denotes modified intermediate neglect of differential overlap) calculations<sup>12</sup> to be more stable by 0.6 eV per surface atom than the site in which Cl interacts with the dimer dangling bond. However, more recent LDA calculations<sup>2</sup> predict the bridge site to be 0.96 eV higher in energy than the dimer site.

With the expectation that Cl bonding would parallel that for H and F, angle-resolved photoemission data from Si(100)2×1-Cl were interpreted on the basis of Cl saturating the dangling bonds.<sup>13</sup> Similarly, a limited set of Cl *K*-edge near-edge surface x-ray-absorption fine-structure (NEXAFS) data were found to be consistent

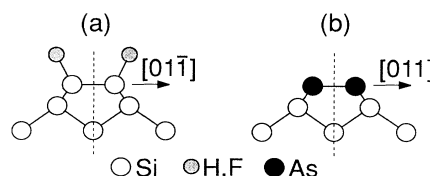


FIG. 1. (a) The symmetric dimer model of Si(100)2×1-F,H; and (b) the As dimer model of Si(100)(1×2)As.

with this geometry.<sup>14</sup> More recently, two independent ESDIAD studies of this surface have been reported,<sup>8,9</sup> with contradictory conclusions. One of these investigations also included high-resolution electron-energy-loss spectroscopy (HREELS) measurements.<sup>8</sup> The ESDIAD and HREELS study<sup>8</sup> proposes a three-center bridge bond configuration at 120 K which irreversibly transforms to a symmetric dimer at about 300 K. The other ESDIAD study<sup>9</sup> concludes that the majority Cl site is atop a buckled dimer.

In this paper we describe a surface structural study of Si(100)2×1-Cl which employed x-ray-absorption spectroscopy (XAS). This follows a brief account of the work in letter form.<sup>10</sup> Here we report in full Cl *K*-edge surface-extended x-ray-absorption fine-structure<sup>15</sup> (SEXAFS) data and near-edge surface x-ray-absorption fine-structure<sup>16</sup> (NEXAFS) results. A prominent white line appears in the Cl *K*-edge NEXAFS data similar to that observed in NEXAFS data of Si(111)7×7-Cl, which has been interpreted in terms of a pseudointramolecular  $\sigma^*$ -type resonance.<sup>10</sup> We employ the polarization dependence of this feature to provide an additional probe of the adsorbate geometry to that obtained from the more conventional structural technique of SEXAFS. In Sec. II we describe the sample characterization and surface x-ray-absorption measurements, the results of which are described in Sec. III. The results are discussed in Sec. IV, where we attempt to resolve the discrepancies in the literature regarding the structure of Si(100)2×1-Cl. Our conclusions are contained in Sec. V.

## II. EXPERIMENTAL DETAILS

Chlorine *K*-edge NEXAFS and SEXAFS data were measured with a Ge(111) crystal pair in the monochromator of station 6.3 at the SRS, Daresbury Laboratory.<sup>17</sup> At the Cl *K* edge (2824 eV) the x-ray beam is close to 100% plane polarized. The Cl *KLL* Auger yield (kinetic energy, 2370 eV) was used as a monitor of the surface absorption coefficient. These measurements employed a double pass cylindrical mirror analyzer (CMA) (Physical Electronics Inc.) operated in the nonretard mode, the CMA axis being parallel to the electric-field vector of the incident radiation. Normalization to the incident x-ray flux was performed by recording the drain current from a thin beryllium foil placed between the monochromator and the sample chamber. NEXAFS were recorded at 5° intervals in the angle of incidence range  $5^\circ \leq \theta \leq 90^\circ$ . Two azimuthal geometries were employed; one in which the x-ray **E** vector was in the [01 $\bar{1}$ ] azimuth, the other having the **E** vector in the [011] azimuth. SEXAFS data were recorded at grazing and normal (or close to normal) photon incidence with the **E** vector in these two azimuths. Measurements were carried out with the sample at room temperature ( $\sim 293$  K) and at a base pressure of  $< 1 \times 10^{-10}$  mbar.

A vicinal  $n^+$ -doped Si(100) wafer cut 4° off the (100) plane towards [011] (arsenic,  $\rho = 4\text{--}6$  m $\Omega$  cm, Wacker-Chemitronic) was used to obtain single-domain surfaces. A nominally flat Si(100) surface consists of two 2×1 domains which lie perpendicular to one another, which can complicate interpretation of experimental data. The

use of a vicinal sample such as that employed here produces, after careful annealing, double atomic-layer steps which result in a single-domain surface.<sup>18</sup> Dimer bonds lie parallel to [01 $\bar{1}$ ], which is termed here the dimer direction. All the angles of incidence given in this paper refer to the [100] direction and not to the macroscopic surface normal.

Samples were cleaned *in situ* by resistive heating up to  $\sim 1100$  K, resulting in surface contamination below the level of detection of Auger electron spectroscopy (AES). The LEED patterns obtained indicated the presence of well-ordered single-domain ( $> 90\%$ ) Si(100)2×1 surfaces.<sup>19</sup> The clean surface was exposed to chlorine by dissociating AgCl in an electrochemical cell,<sup>20</sup> the sample being maintained at  $\sim 500$  K during exposure to ensure that weakly bound chloride phases were not formed on the surface.<sup>21</sup> This method was preferred over the alternative approach of adsorption at lower temperature followed by annealing since it avoids the possibility of water contamination from the residual vacuum. This can be problematic since the sticking coefficient for H<sub>2</sub>O on Si(100)2×1 is close to unity at room temperature.<sup>22</sup> Clean surface LEED patterns were retained after chlorine exposure with the appearance of some additional intensity in the Si(100)2×1 [011]-direction half-order beams. For comparison, NEXAFS data were also recorded from a Si(100) surface exposed to chlorine at room temperature.

## III. RESULTS

### A. SEXAFS

Figure 2 compares Cl *KLL* Auger yield Cl *K*-edge SEXAFS data obtained at grazing and near-normal incidence in the [011] azimuth and at normal incidence in the [01 $\bar{1}$ ] azimuth. Background subtraction and normalization of the grazing incidence Auger yield data to the edge jump yields the EXAFS oscillations  $\chi(k)k^2$  and their Fourier transform shown as solid lines in Fig. 3. This EXAFS spectrum was analyzed using EXCURV90, a curve-fitting procedure based on the rapid curved wave computational scheme.<sup>23</sup> Analysis employed phase shifts and backscattering amplitudes obtained from Cl *K*-edge EXAFS data from SiCl<sub>4</sub>,<sup>24</sup> in which the Si-Cl distance is  $2.018 \pm 0.003$  Å.<sup>25</sup> The data can be adequately modeled with a single Si backscattering shell. The best fit to the experimental data, after constraining the Debye-Waller-like factor to a physically reasonable value ( $2\sigma^2 = 0.005$  Å<sup>2</sup>) is compared with experiment in Fig. 3. This corresponds to a Cl-Si bond distance of  $2.00 \pm 0.02$  Å and an effective coordination number of 2.6. No evidence of any EXAFS was found in normal incidence data recorded with the x-ray **E** vector in either the [01 $\bar{1}$ ] or the [011] azimuth.

### B. NEXAFS

Figure 4 shows the Cl *K*-edge NEXAFS data recorded as a function of incidence angle with the x-ray **E** vector in the two azimuths of Si(100)2×1-Cl. The data have been

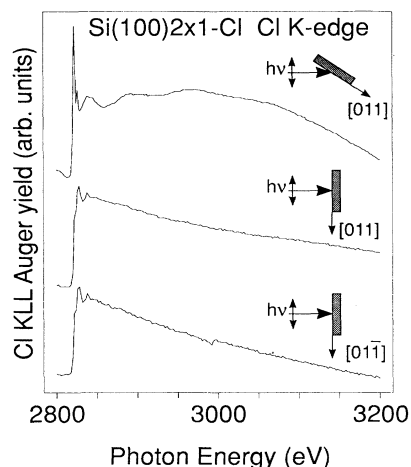


FIG. 2. Cl *KLL* Auger yield at the Cl *K* edge from Si(100)2×1-Cl. Data were recorded at an angle of incidence of 6° (grazing) and 84° (near-normal) with the x-ray **E** vector in the [011] azimuth and at 90° (normal) with the **E** vector in the [01 $\bar{1}$ ] azimuth. Angles refer to those between the **E** vector and [100], not the macroscopic surface normal. The feature at 2995 eV in the lower spectrum arises from a third-order (800) Bragg reflection in the substrate. The edge step in the 6° (84°) [011] azimuth data is 0.42 (0.75), that in the normal-incidence [01 $\bar{1}$ ] azimuth data being 0.78 (Ref. 29).

normalized to the absorption-edge step. The white line at  $\sim 2822$  eV is seen to increase in intensity as the photon incidence angle becomes more grazing in both azimuths.

The NEXAFS spectra in Fig. 4 are very similar to those recorded from Si(111)7×7-Cl, especially in the region around the white line.<sup>10</sup> This feature in Si(111)7×7-Cl data, which lies  $\sim 5$  eV above the absorption edge, has been assigned to a transition between Cl *1s*

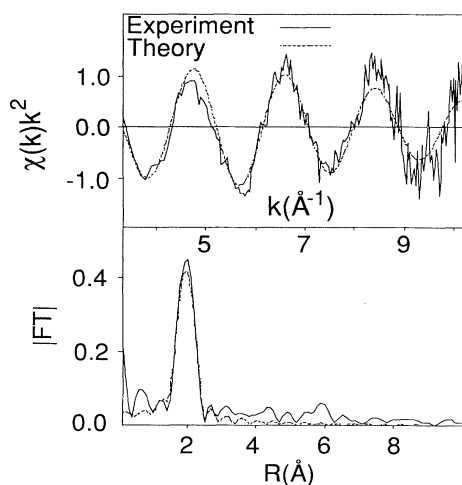


FIG. 3. Cl *KLL* Auger yield Cl *K*-edge SEXAFS spectra from Si(100)2×1-Cl recorded at an angle of incidence of 6° with the x-ray **E** vector in the [011] azimuth. The EXAFS function  $\chi(k)$  weighted by  $k^2$  (solid line) and the best fit (dashed line) are compared in the upper part of the figure. The corresponding lower section contains the modulus of the Fourier transform.

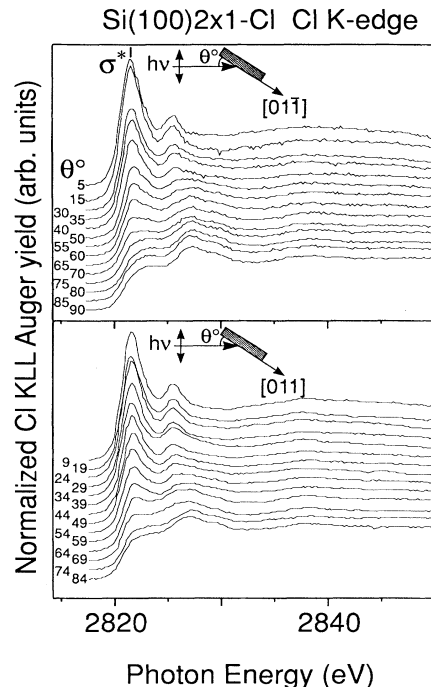


FIG. 4. Cl *K*-edge Cl *KLL* Auger yield NEXAFS from Si(100)2×1-Cl as a function of x-ray incidence angle,  $\theta$ , with the **E** vector in the [01 $\bar{1}$ ] and [011] azimuths. The pseudointramolecular  $\sigma^*$  resonance is indicated.

and predominantly (Cl,Si) *3p*-derived  $\sigma_z^*$  states.<sup>10,26</sup> The polarization dependence of this *1s*→ $\sigma^*$  resonance displays pseudointramolecular behavior.<sup>10</sup> In other words, it behaves in a manner similar to that observed for molecular NEXAFS resonances,<sup>16</sup> and as such the polarization dependence can be used to gain information about the orientation of the Cl-Si bond. For Si(111)7×7-Cl, in which the Si-Cl bond lies along the surface normal,<sup>10,26</sup> the resonance goes to zero at normal incidence, as expected from dipole selection rules.<sup>16</sup>

The similarity of the Cl *K*-edge NEXAFS spectra of Si(100)2×1-Cl and Si(111)7×7-Cl data is consistent with pseudointramolecular behavior, being dominated by short-range scattering. Analysis of the Si(100)2×1-Cl data employed the same methods as those used to analyze the Si(111)7×7-Cl spectra, which followed procedures adopted for molecular resonances.<sup>16,27</sup> This involved isolating the  $\sigma^*$  resonance by subtraction of an arctangent function, set up to model the absorption edge. The parameters were established by fitting the function to normal-incidence data, where there is a negligible contribution from the resonance. A second method was employed which involved subtraction of normal-incidence data. The intensity of the resonance was subsequently obtained by fitting the isolated resonance to a symmetric Gaussian. The background and Gaussian-fitting procedures are illustrated in Fig. 5 using Si(111)7×7-Cl data as examples. While the result of both methods was essentially the same, we show results derived from subtraction of normal-incidence data, since this procedure involves

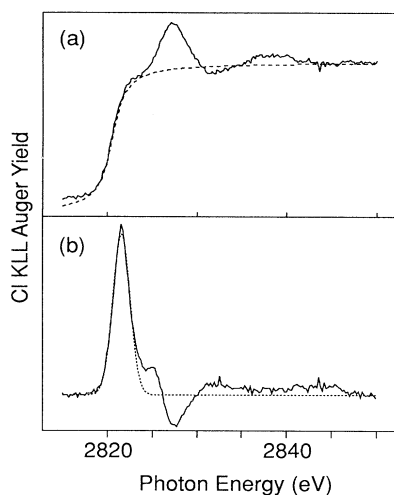


FIG. 5. An illustration of the methods used to obtain the area of the  $\sigma^*$  Cl *K*-edge resonance in NEXAFS spectra of chlorine adsorbed on Si surfaces. (a) The use of an arctangent function to fit the absorption-edge step in the normal-incidence spectrum of Si(111)7 $\times$ 7-Cl. (b) Fitting the  $\sigma^*$  resonance to a Gaussian function in the 55° angle of incidence spectrum of Si(111)7 $\times$ 7-Cl. The arctangent function obtained in (a) has been subtracted from the spectrum.

fewer fitting parameters.

The data in Fig. 6 indicate that the polarization dependence is the same in both azimuths, and follows that observed for Si(111)7 $\times$ 7-Cl. This similarity extends to the three data sets having comparable edge-step-normalized peak areas at all angles of x-ray incidence. This is evidenced in Fig. 6, where we compare the  $a \cos^2\theta$  fit to the Si(111)7 $\times$ 7-Cl data with the Si(100)2 $\times$ 1-Cl experimental values.

Normal-incidence NEXAFS data recorded with the **E** vector in the [01 $\bar{1}$ ] azimuth from a surface prepared by room-temperature dosing are compared with annealed-surface spectra in Fig. 7. This comparison shows that the intensity of the  $\sigma^*$  resonance in the unannealed surface is comparable with that in the spectrum recorded at an angle of incidence of 70° from the annealed surface.

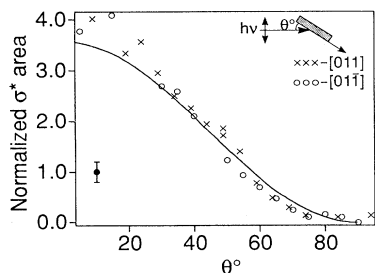


FIG. 6. The edge-step-normalized Gaussian area of the Cl *K*-edge  $\sigma^*$  resonance from Si(100)2 $\times$ 1-Cl ([011] azimuth, crosses; [01 $\bar{1}$ ] azimuth, open circles). The solid line shows the result of a least-squares fit of Si(111)7 $\times$ 7-Cl data to the function  $a \cos^2\theta$ .

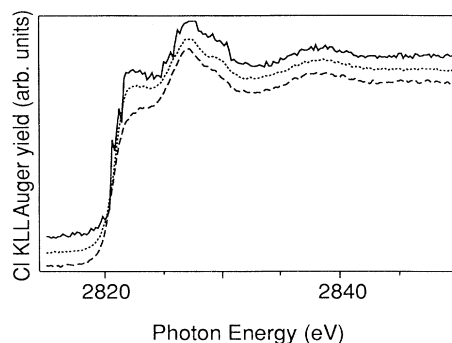


FIG. 7. A comparison of Cl *K*-edge NEXAFS spectra of Si(100)2 $\times$ 1-Cl recorded with the x-ray **E** vector in the [01 $\bar{1}$ ] azimuth. Data recorded from an unannealed surface prepared at room temperature at normal incidence (solid line); and from a surface prepared by 500-K dosing at an angle of incidence of 70° (dotted line) and 90° (dashed line).

#### IV. DISCUSSION

The SEXAFS results described above are consistent with the Si-Cl bond lying within 10° of the [100] direction. This accounts for the lack of backscattering at normal incidence and the effective coordination number derived from grazing incidence data. The effective coordination number obtained from data recorded at an angle of incidence of 6° with the **E** vector in the [011] azimuth, 2.6, compares with the value expected for atop Cl of 2.9. This discrepancy is well within the accepted errors for coordination numbers.<sup>15</sup> The NEXAFS results shown in Fig. 6 indicate that the  $\sigma^*$  resonance has a  $\cos^2\theta$  polarization dependence in both azimuthal geometries. Hence the NEXAFS data also support an atop Cl site.

The Si-Cl bond distance derived from the SEXAFS data,  $2.00 \pm 0.02$  Å, is identical to that found for Si(111)7 $\times$ 7-Cl.<sup>26</sup> The superior quality of the present data leads to a better estimate of the bond distance than that previously reported for the (100) surface,  $1.95 \pm 0.04$  Å.<sup>14</sup> This Si-Cl bond length is similar to that found in molecular systems; across the series SiCl<sub>4</sub>, SiCl<sub>3</sub>H, SiCl<sub>2</sub>H<sub>2</sub>, and SiClH<sub>3</sub>, the bond length is essentially invariant [Cl-Si bond length of  $2.035 \pm 0.020$  Å (Ref. 28)].

Since XAS does not provide the full surface structure, we must turn to other measurements to assess the position of the Si-Cl bond in relation to the underlying substrate. A key parameter is the Cl coverage, where we define 1 monolayer (ML) as corresponding to the density of individual surface-layer Si atoms on a particular Si face, i.e., (100) or (111). In this work the  $\text{Cl}_{\text{LMM}}/\text{Si}_{\text{LMM}}$  AES ratio recorded from freshly formed Si(100)2 $\times$ 1-Cl was found to be  $\sim 0.6$  when care was taken to avoid electron-stimulated desorption effects. This value decreased to  $\sim 0.4$  after several hours in the x-ray beam due to photon-stimulated desorption. Here we do not attempt to employ the absolute value of the AES ratio, but instead compare it with that obtained from Si(111)7 $\times$ 7-Cl. We find the AES ratio of the two surfaces to be comparable when Si(111)7 $\times$ 7-Cl is prepared in a manner

similar to that used to form Si(100)2×1-Cl. Furthermore, without any adjustments to the experimental setup between measurements on the two surfaces, the relative edge jump<sup>29</sup> of the Cl *KLL* Auger yield through the Cl *K* edge was found to be the same for corresponding experimental geometries (~70% at normal incidence and ~40% at grazing incidence). The obvious conclusion is that the concentration of Cl on the two surfaces is comparable.

We can now assess the absolute coverage on Si(100)2×1 by comparison with that on Si(111)7×7, based on the assumption that the saturated Cl coverage on our Si(111)7×7-Cl reference surface is close to 1 ML. The Cl density on the Si(111)7×7-Cl surface, corresponding to one Cl atom per adatom,<sup>26</sup> is ~52 Å<sup>-2</sup>. Using the AES and absorption-edge step data then indicates a Cl coverage on our Si(100)2×1-Cl surface of ~0.25 ML, since the unit-cell area on Si(100)2×1 (the area per dimer) is ~29 Å<sup>2</sup>. Moreover, the AES ratio of 0.6 for the (100) surface is consistent with a coverage of ~0.25 ML by comparison with the results of Gao *et al.*,<sup>8</sup> who used a calibrated dosing source. We believe that this provides a better estimate of the coverage than that previously employed by us,<sup>13</sup> where we simply used the ratio of AES peaks to obtain a coverage of ~1 ML on the (100) surface.

We now turn to the effect of Cl adsorption on the LEED pattern. Although the majority 2×1 domain pattern is maintained, the small increase observed in the minority domain half-order LEED spots suggests that etching of the surface may have occurred. There is an alternative explanation for the modification of the LEED pattern, which involves the formation of Cl-Cl dimers in the [011] direction, paralleling the behavior of As.<sup>5</sup> However, this can be ruled out by the absence of Cl backscattering in the normal-incidence SEXAFS recorded with the *E* vector in the [011] azimuth. The lack of quantitative LEED measurements prevents us from distinguishing partial deconstruction of the 2×1 surface or the random occupation of an adsorption site. The former effect would be apparent as a decrease in intensity of ½-order beams, the latter as an increase in the diffuse background. However, it seems unlikely that Cl lifts the 2×1 reconstruction by breaking the dimer bonds, since the Si-Cl bonds formed are expected to lie ~55° from [100] at low coverage, by comparison with predictions for Si(100)2×1-F.<sup>30</sup>

The evidence for etching might support the idea that Cl atoms are only bound to step sites.<sup>31,32</sup> In principle, etching could double the step density of the vicinal surface by producing monatomic steps. In this limit, where a two-domain surface is produced, the maximum step-site Cl coverage is about 0.1 ML, assuming one Cl per dimer at the step.<sup>5</sup> The latter condition is required in order that the bond geometry is consistent with the XAS data (see below). Both the AES ratio and the absorption-edge steps appear too large to be consistent with 0.1-ML coverage. Moreover, our LEED data indicate that the two-domain limit is not approached, further lowering the coverage in the step-site model. We take the above to indicate that Cl atoms are bound to dimer atoms

on terraces and possibly at steps.

In considering possible structural models, we take account of the orientation of the Si-Cl bond (parallel to [100]), the coverage (≤0.25 ML), and the LEED pattern (2×1). We first consider models in which two Cl atoms are bound to each dimer, recognizing that islanding would be required in order to make such a model consistent with the coverage. The XAS data are clearly not consistent with the structural model of Si(100)2×1-Cl which contains symmetric Si dimers with one Cl atom at each end of the dimer. In this model the Si-Cl bond is expected to lie ~20° from [100].<sup>2</sup> If for some reason the bond was within 10° of [100], consistent with the NEXAFS and first-shell SEXAFS, then Cl backscattering would be detected in the normal-incidence SEXAFS. The possibility that Cl atoms bond at both ends of a buckled dimer is not thought to represent a realistic option when coupled with the known Si-Cl bond orientation.

For one Cl bound to each dimer there are three high-symmetry structures possible. The dimer bridge site is ruled out by the XAS-derived Si-Cl bond orientation. Cl bound to one end of a symmetric dimer is unlikely to be stable given the asymmetry introduced by Cl,<sup>33</sup> and tends to be excluded by the expected Si-Cl alignment. The final site, and that preferred here, has Cl bonded atop the upper Si atom of a buckled dimer, as shown in Fig. 8. With all such sites occupied in a 2×1 reconstruction, Cl backscattering should be detected in the normal-incidence SEXAFS recorded with the *E* vector in the [011] azimuth. In this geometry, the effective coordination number of Cl would be 6 and the bond distance would be 3.84 Å. However, at 0.25-ML coverage and random site occupation, the effective coordination number reduces to 1.3. This is entirely consistent with the lack of fine structure in the normal-incidence SEXAFS.

We have two other structural studies of Si(100)2×1-Cl with which to compare our results. Both of these studies employed ESDIAD. The structural model deduced above is consistent with the ESDIAD results of Bennett, Greenwood, and Williams.<sup>9</sup> They observed principally normal emission of Cl<sup>+</sup> ions from Si(100)2×1-Cl when they employed the same preparative method as that used in the current work. Off-normal emission beams were observed in the case of a vicinal substrate after chlorine adsorption at room temperature, consistent with our NEXAFS results obtained from a similarly prepared sur-

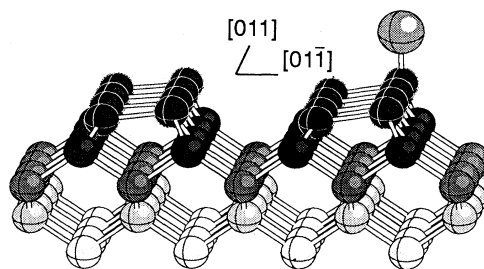


FIG. 8. The proposed bonding site for Cl on the upper Si atom of a Si(100)2×1 buckled dimer.

face. The off-normal beams were ascribed to either emission from both ends of a symmetric dimer or from polychloride species.

In contrast, another ESDIAD study<sup>8</sup> produced very different conclusions. Here Cl<sub>2</sub> adsorption and ESDIAD measurements were performed at 120 K, and the effect of annealing the surface was investigated. Normal Cl<sup>+</sup> emission was obtained without annealing, and assigned to desorption from bridge sites. Off-normal beams, consistent with desorption from both ends of a symmetric dimer, were observed to increase in intensity relative to the central beam on annealing the surface to temperatures lower than 700 K. At higher anneal temperatures emission is again dominated by a central beam, ascribed to desorption from randomly oriented Si-Cl bonds formed during etching. The results described above were obtained following an initial coverage of  $\sim 0.7$  ML.<sup>8</sup> Since there was no significant thermal desorption from a surface with this coverage up to 700 K,<sup>8</sup> the same coverage will apply to the annealed surfaces.

There are a number of possible reasons for the apparent discrepancies between the ESDIAD and HREELS result<sup>8</sup> on the one hand and the ESDIAD results of Bennett, Greenwood, and Williams<sup>9</sup> and our XAS results on the other. These are most obviously the following: the coverages employed, the use of a planar as opposed to a vicinal substrate, and dosing from bottled gas as opposed to an electrochemical cell. The latter factor could be important if there was a significant atomic Cl contribution to the output from the cell, since atomic and molecular chlorine are known to reach very differently.<sup>34</sup> However, Jackman, Ebert, and Foord<sup>21</sup> obtained the same temperature-programmed desorption (TPD) results when employing either source of chlorine. This tends to rule out the source of chlorine as the origin of the discrepancy.

The use of a vicinal substrate with a high step density in the current work might be expected to promote etching, lowering the temperature at which it takes place. As noted above, a small degree of etching is detected in our LEED pattern, but it exposes an ordered array of dimers in the second layer, not a disordered substrate. Furthermore, Bennett, Greenwood, and Williams<sup>9</sup> obtain comparable results from planar and vicinal substrates. In addition, our XAS data are not consistent with a disordered array of Si-Cl bonds. This strongly suggests that the step density does not play a key role in determining the different behavior observed.

As for the coverage, it is clear that the structural model derived from XAS is inconsistent with the coverage of 0.7 ML attained in the ESDIAD and HREELS work.<sup>8</sup> In our XAS-derived model the most likely consequence of increasing the coverage beyond 0.5 ML, where all single-Cl-bonded dimers are saturated, would be to form dimers to which two Cl atoms were bound. The ESDIAD pattern should then consist of a central beam from Cl on buckled dimers and off-normal beams from symmetric dimers, with an intensity ratio dictated by the desorption cross section as well as the coverage. Such a pattern is not inconsistent with the ESDIAD results obtained from the 0.7-ML-covered surface annealed to 523

K.<sup>8</sup> This interpretation was discounted<sup>8</sup> on the grounds that the beams from buckled dimers are expected to lie 8° off normal (which is within the error of the XAS-derived angle). However, this figure is an estimate only. Below a certain angle of the Si-Cl bond away from [100], ESDIAD would not resolve the four Cl<sup>+</sup> beams arising from off-normal emission. Some support for this means of reconciling the ESDIAD and XAS data is gained by considering the effect on the ESDIAD image of reducing the initial coverage.<sup>8</sup> It is particularly notable that the ratio of off-normal to normal beam intensity sharply decreases on reducing the coverage to below 0.5 ML. Given these arguments, it seems that differences in the Cl coverage provides a plausible explanation for the discrepancies between the ESDIAD and XAS results obtained from surfaces annealed to  $\sim 500$  K. It does rely, however, on the cross section for off-normal emission being considerably higher than that for the central beam. This follows from the presence of off-normal emission in the ESDIAD image from a 0.35-ML surface after annealing to 673 K.<sup>8</sup>

As for species formed at room temperature and below, the interpretation above does not preclude the presence of dimer-bridging Cl species, as proposed in the ESDIAD and HREELS work.<sup>8</sup> The suggestion that this irreversibly transforms to terminal dimer sites on raising the temperature to 300 K is also not inconsistent with the other ESDIAD study<sup>9</sup> and our NEXAFS data from an unannealed surface recorded with the *E* vector in the [01 $\bar{1}$ ] azimuth. The latter surface was prepared with the same coverage ( $\leq 0.25$  ML) as the surfaces formed by exposure at 500 K. The NEXAFS data could be interpreted as evidencing Cl bonding at both ends of a symmetric dimer, with a Si-Cl bond  $\sim 20^\circ$  from [100]. Indeed, this is favored over the alternative interpretation, that of the formation of higher chlorides by breaking dimer bonds. This follows from the absence of a 550-K SiCl<sub>4</sub> desorption peak in TPD spectra from a surface having a Cl coverage  $< 0.25$  ML.<sup>8</sup> If this were the case, it would suggest that Cl<sub>2</sub> dissociation on the room-temperature surface is local to one dimer.

## V. CONCLUSIONS

In this surface x-ray-absorption study of Si(100)2 $\times$ 1-Cl, the Si-Cl bond is found to lie within 10° of the surface normal. This figure, which applies to a surface formed at  $\sim 500$  K with a Cl coverage of about 0.25 ML, is derived from polarization-dependent Cl *K*-edge SEXAFS. The polarization dependence of the pseudointramolecular  $\sigma^*$  NEXAFS resonance is consistent with this geometry. Normal-incidence XAS data show no distinguishable EXAFS. The Si-Cl bond geometry, the coverage, and the absence of major changes to the 2 $\times$ 1 LEED pattern on Cl adsorption are used to derive the surface structure. This has Cl bonded atop the upper Si atom of a buckled dimer, with random occupation of these sites on terraces and possibly steps.

The XAS results are consistent with ESDIAD data from a surface prepared in a similar manner,<sup>9</sup> but the conclusions of these two studies differ from those of an

ESDIAD and HREELS investigation.<sup>8</sup> A plausible explanation for the discrepancies is associated with the coverage employed, with some Cl atoms bound to both ends of symmetric dimers at higher coverage.

Adsorption of Cl<sub>2</sub> at room temperature to a Cl coverage of about 0.25 ML also appears to result in a symmetric dimer geometry. This is taken to indicate that Cl<sub>2</sub> dissociates about a single dimer at room temperature, with thermally activated formation of the lower-energy buckled dimer configuration. However, further structural

studies are required to fully define the temperature and coverage dependence.

#### ACKNOWLEDGMENTS

We thank Dr. R. I. G. Uhrberg for the sample used in this study and Professor J. T. Yates for providing us with copies of his work prior to its publication. This work was funded by the United Kingdom Science and Engineering Research Council, with additional support from Johnson Matthey Plc.

\*Present address: IBM Research Division, Zurich Research Laboratory, Säumerstrasse 4, CH-8803 Rüschlikon, Switzerland.

†Present address: Département de Chimie Appliquée et Génie Chimique, CNRS URP, 43, Bd. du 11 Novembre 1918, F-69622 Villeurbanne CEDEX, France.

‡Present address: Xenolith, 318 10th Ave. East, Seattle, WA 98102.

<sup>1</sup>R. A. Wolkow, Phys. Rev. Lett. **68**, 2636 (1992).

<sup>2</sup>P. Krüger and J. Pollmann, Phys. Rev. B **47**, 1898 (1993).

<sup>3</sup>R. I. G. Uhrberg and G. V. Hansson, Crit. Rev. Solid State Mater. Sci. **17**, 133 (1991).

<sup>4</sup>R. G. Jones, Prog. Surf. Sci. **27**, 25 (1988).

<sup>5</sup>R. D. Bringans, R. I. G. Uhrberg, M. A. Olmstead, and R. Z. Bachrach, Phys. Rev. B **34**, 7447 (1986).

<sup>6</sup>J. J. Boland, Phys. Rev. Lett. **67**, 1539 (1991); **67**, 2591 (1991).

<sup>7</sup>M. J. Bozack, M. J. Dresser, W. J. Choyke, P. A. Taylor, and J. T. Yates, Surf. Sci. **184**, L332 (1987).

<sup>8</sup>C. C. Cheng, Q. Gao, W. J. Choyke, and J. T. Yates, Phys. Rev. B **46**, 12 810 (1992); Q. Gao, C. C. Cheng, P. J. Chen, W. J. Choyke, and J. T. Yates, J. Chem. Phys. **98**, 8308 (1993).

<sup>9</sup>S. L. Bennett, C. L. Greenwood, and E. M. Williams, Surf. Sci. (to be published).

<sup>10</sup>D. Purdie, C. A. Muryn, N. S. Prakash, K. G. Purcell, P. L. Wincott, G. Thornton, and D. S.-L. Law, J. Phys. Condens. Matter **3**, 7751 (1991).

<sup>11</sup>T. Weser, A. Bogen, B. Konrad, R. D. Schnell, C. A. Schug, and W. Steinmann, Phys. Rev. B **35**, 8184 (1987).

<sup>12</sup>B. I. Craig and P. V. Smith, Surf. Sci. **262**, 235 (1992).

<sup>13</sup>L. S. O. Johansson, R. I. G. Uhrberg, R. Lindsay, P. L. Wincott, and G. Thornton, Phys. Rev. B **42**, 9534 (1990).

<sup>14</sup>G. Thornton, P. L. Wincott, R. McGrath, I. T. McGovern, F. M. Quinn, D. Norman, and D. D. Vvedensky, Surf. Sci. **211/212**, 959 (1989).

<sup>15</sup>For a review see P. H. Citrin, J. Phys. (Paris) Colloq. **47**, C8-437 (1986).

<sup>16</sup>For a review see J. Stöhr, in *NEXAFS Spectroscopy*, edited by R. Gomer, Springer Series in Surface Sciences Vol. 25 (Springer-Verlag, Berlin, 1992).

<sup>17</sup>A. A. MacDowell, D. Norman, and J. B. West, Rev. Sci. Instrum. **57**, 2667 (1986).

<sup>18</sup>J. E. Griffith and G. P. Kochanski, Crit. Rev. Solid State Mater. Sci. **16**, 255 (1990).

<sup>19</sup>R. Kaplan, Surf. Sci. **93**, 145 (1980).

<sup>20</sup>The chlorine source is a modified version of the design described in N. D. Spencer, P. J. Goddard, P. W. Davies, M. Kitson, and R. M. Lambert, J. Vac. Sci. Technol. A **1**, 1554 (1983).

<sup>21</sup>R. B. Jackman, H. Ebert, and J. S. Foord, Surf. Sci. **176**, 183 (1986).

<sup>22</sup>E. Schröder-Bergen and W. Ranke, Surf. Sci. **236**, 103 (1990).

<sup>23</sup>S. J. Gurman, N. Binstead, and I. Ross, J. Phys. C **17**, 143 (1984).

<sup>24</sup>W. Myring and G. Thornton (unpublished).

<sup>25</sup>R. R. Ryan and K. Hedberg, J. Chem. Phys. **50**, 4986 (1969).

<sup>26</sup>P. H. Citrin, J. E. Rowe, and P. Eisenberger, Phys. Rev. B **28**, 2299 (1983).

<sup>27</sup>D. A. Outka and J. Stöhr, J. Chem. Phys. **88**, 3539 (1988).

<sup>28</sup>*Tables of Interatomic Distances and Configurations in Molecules and Ions*, edited by L. E. Sutton, Special Publication No. 18 (The Chemical Society, London, 1965).

<sup>29</sup>The edge step is defined here as the difference in count rate above and below the absorption edge divided by the count rate below the edge.

<sup>30</sup>C. J. Wu and E. A. Carter, Phys. Rev. B **45**, 9065 (1992).

<sup>31</sup>N. Aoto, E. Ikawa, T. Kikkawa, and Y. Kurogi, Surf. Sci. **250**, 235 (1991).

<sup>32</sup>N. Aoto, E. Ikawa, and Y. Kurogi, Surf. Sci. **199**, 408 (1988).

<sup>33</sup>M. Tsuda, T. Hoshino, S. Oikawa, and I. Ohdomari, Phys. Rev. B **44**, 11 241.

<sup>34</sup>J. Matsuo, K. Karahashi, A. Sato, and S. Hijiya, Jpn. J. Appl. Phys. **31**, 2025 (1992).